



Published in final edited form as:

*Int J Cardiol.* 2016 November 1; 222: 361–367. doi:10.1016/j.ijcard.2016.07.263.

## Apelin-13 infusion salvages the peri-infarct region to preserve cardiac function after severe myocardial injury

Wook-Jin Chung<sup>a,b,c</sup>, Ahryon Cho<sup>d</sup>, Kyunghee Byun<sup>c,e,f</sup>, Jeongsik Moon<sup>c,f</sup>, Xiaohu Ge<sup>a</sup>, Hye-Sun Seo<sup>g</sup>, Ejung Moon<sup>h</sup>, Rajesh Dash<sup>a</sup>, and Phillip C. Yang<sup>\*,a</sup>

<sup>a</sup> Department of Cardiovascular Medicine, Stanford University, Stanford, CA, USA

<sup>b</sup> Department of Cardiovascular Medicine, Gachon University, Incheon, Republic of Korea

<sup>c</sup> Gachon Cardiovascular Research Institute, Gachon University, Incheon, Republic of Korea

<sup>d</sup> Department of Pathology, Stanford University, Stanford, CA, USA

<sup>e</sup> Department of Anatomy and Cell Biology, Gachon University, Incheon, Republic of Korea

<sup>f</sup> Center for Genomics and Proteomics & Stem Cell Core Facility, Lee Gil Ya Cancer and Diabetes Institute, Gachon University, Incheon, Republic of Korea

<sup>g</sup> Division of Cardiology, Soon Chun Hyang University College of Medicine, Bucheon, Republic of Korea

<sup>h</sup> Department of Radiation Oncology, Stanford University, Stanford, CA, USA

### Abstract

**Background**—Apelin-13 (A13) regulates cardiac homeostasis. However, the effects and mechanism of A13 infusion after an acute myocardial injury (AMI) have not been elucidated. This study assesses the restorative effects and mechanism of A13 on the peri-infarct region in murine AMI model.

**Methods**—51 FVB/N mice (12 weeks, 30 g) underwent AMI. A week following injury, continuous micro-pump infusion of A13 (0.5 µg/g/day) and saline was initiated for 4-week duration. Dual contrast MRI was conducted on weeks 1, 2, 3, and 5, consisting of delayed-enhanced and manganese-enhanced MRI. Four mice in each group were followed for an extended period of 4 weeks without further infusion and underwent MRI scans on weeks 7 and 9.

**Results**—A13 infusion demonstrated preserved LVEF compared to saline from weeks 1 to 4 ( $21.9 \pm 3.2\%$  to  $23.1 \pm 1.7\%$  vs.  $23.5 \pm 1.7\%$  to  $16.9 \pm 2.8\%$ ,  $*p = 0.02$ ), which persisted up to 9 weeks post-MI ( $+1.4\%$  vs.  $-9.4\%$ ,  $*p = 0.03$ ). Mechanistically, dual contrast MRI demonstrated significant decrease in the peri-infarct and scar % volume in A13 group from weeks 1 to 4 ( $15.1$  to  $7.4\%$  and  $34.3$  to  $25.1\%$ ,  $p = 0.02$ , respectively). This was corroborated by significant increase in 5-ethynyl-2'-deoxyuridine (EdU<sup>+</sup>) cells by A13 vs. saline groups in the peri-infarct region ( $16.5$

\* Corresponding author at: Medicine (Cardiovascular Medicine), 269 Campus Drive, CCSR 3115C, Stanford, CA 94305, USA. phillip@stanford.edu (P.C. Yang).

Conflict of interest

The authors report no relationships that could be construed as a conflict of interest.

$\pm 3.1\%$  vs.  $8.1 \pm 1.6\%$ ;  $p = 0.04$ ), suggesting active cell mitosis. Finally, significantly enhanced mobilization of CD34<sup>+</sup> cells in the peripheral blood and up-regulation of APJ, fibrotic, and apoptotic genes in the peri-infarct region were found.

**Conclusions**—A13 preserves cardiac performance by salvaging the peri-infarct region and may contribute to permanent restoration of the severely injured myocardium.

## Keywords

Apelin-13; Myocardial infarction; Stem cell; Magnetic resonance imaging; Salvage

## 1. Introduction

Coronary artery disease continues to carry high mortality and morbidity despite introduction of novel therapeutics, including stem cell therapy [1–3]. Although recent clinical stem cell trials showed promise in ischemic cardiomyopathy, there are still many unresolved debates regarding the ideal cell-type, mode of delivery, restorative effects, and mechanism of repair [2–4].

Apelin-13 (A13) is a recently discovered endogenous peptide associated with G-protein coupled receptor APJ in both human and murine species [5]. A13 is a potent inotropic and vasodilatory agent, demonstrating the beneficial preclinical effects in myocardial injury models [6–8]. In addition, the Apelin-APJ system influences the heart field development and cardiac differentiation of pluripotent stem cells as we have reported recently [9,10]. Other groups have reported that A13 may modulate endogenous stem cell function after acute myocardial injury (AMI) [11,12]. However, there is no definitive tissue characterization of the restorative effects on the injured myocardium. Moreover, the potential mechanisms underlying A13, including mobilization of bone marrow derived stem cells (BMSCs) and cardiac stem cells (CSCs), have not been delineated.

Precise characterization of the myocardium is critical to understand the impact of A13 on cardiac function and remodeling. The gold standard for infarct evaluation, delayed-enhancement MRI (DEMRI), using gadolinium (Gd<sup>2+</sup>)-based contrast agent does not provide direct cell viability information because of its non-specific distribution in the extra-cellular space and does not delineate the peri-infarct region [13–16]. On the other hand, manganese-enhanced MRI (MEMRI), a viability-specific contrast agent, employing Mn<sup>2+</sup>-based contrast agent enters only the viable cells via voltage-gated calcium channels [13]. Used in combination, MEMRI-positive viable myocardium overlaps the DEMRI-positive injured myocardium to generate a clear delineation of at-risk but viable peri-infarct myocardium as we have described previously [14].

This study hypothesizes that A13 salvages the injured myocardium through direct effects on the peri-infarct region by mobilization of BMSCs and up-regulation of LV remodeling genes. Specifically, dual contrast cardiac MRI studies assess the restorative effects of A13 on the peri-infarct region in murine AMI model.

## 2. Methods

### 2.1. Murine myocardial injury model

All animal studies were approved by the Stanford University Administrative Panel on Laboratory Animal Care. Animals were housed in a temperature-controlled ( $20 \pm 2^\circ\text{C}$ ) and humidity-controlled (60%) room under a 12 h light/cycle 6:00 am/6:00 pm. Male FVB/N mice at 12–14 weeks (Charles River Inc., Hollister, CA) were used.

Myocardial injury and MRI were performed in a total of 51 adult FVB/N mice (Fig. 1) [5]. Briefly, the mice were anesthetized with 2–3% inhalational isoflurane and intraperitoneal sodium pentobarbital. They were intubated to achieve positive pressure ventilation with oxygen/isoflurane mixture and thoracotomy was performed. Peak inspiratory pressure was maintained between 10 and 14 cm H<sub>2</sub>O. The lung was retracted and the pericardium was incised. The left anterior descending (LAD) coronary artery was ligated until blanching of the distal left ventricle. Following complete hemostasis, the chest wall was closed in four layers. The animal was weaned from the ventilator, extubated, and monitored in the recovery area. Thirty-two of 51 (35% mortality,  $n = 19$ ) mice were randomly assigned to either apelin-13-treated group or NS (normal saline) control group at the time of micro-pump insertion at 1 week after AMI.

### 2.2. Continuous systemic administration of A13 and NS using micro-osmotic pump

Half-life of A13 is approximately 30 min, requiring continuous micro-osmotic infusion pump (0.25  $\mu\text{L/h}$ , 14 days; Alzet Direct, Cupertino, CA) of A13 (0.5  $\mu\text{g/g/day}$ ; American Peptide, Sunnyvale, CA) and NS for 4-week duration, following 1 week of convalescence post-LAD ligation in A13 treatment ( $n = 16$ ) and in NS control ( $n = 16$ ) groups [8]. The animals underwent DEMRI and MEMRI on consecutive days at 1, 2, 3 and 5 weeks after AMI. A subset of mice was followed for an extended period from weeks 6 to 9 without any treatment ( $n = 4$  per group), additional scans were performed on weeks 7 and 9. All mice ( $n = 3$  per group at week 2;  $n = 8$  per group at week 5; and  $n = 4$  per group at week 9) were sacrificed to perform ex vivo assays on explanted heart tissue.

### 2.3. In vivo MEMRI and DEMRI

To prepare for scanning, anesthesia was induced with 2% and maintained with 1.25–1.5% isoflurane. ECG leads were inserted subcutaneously to assess the heart rate while the body temperature was maintained at  $37^\circ\text{C}$  and respiratory rate was monitored. Using a 3T GE Signa Excite whole-body scanner with a dedicated mouse coil (Rapid MR International, Germany), multiple cardiac function parameters were obtained on weeks 1, 2, 3 and 5 after AMI and additionally on weeks 7 and 9 for the extended survival group without the infusion treatment. The following sequences were performed for MRI acquisitions: (1) DEMRI — IP injection of 0.2 mmol/kg gadopentetate dimeglumine (Magnevist, Berlex Laboratories) and EKG gated fast gradient echo inversion recovery (fGRE-IR) sequences with FOV 4 cm, slice thickness 1 mm, matrix  $256 \times 256$ , TE 5 ms, TI 200–300 ms, NEX 2, and FA  $30^\circ$  and (2) MEMRI — IP injection of 0.7 cc/kg of manganese contrast agent (EVP1001-1, Eagle Vision Pharmaceutical) and EKG gated fGRE-IR sequence with FOV 4 cm, slice thickness 1 mm, matrix  $256 \times 256$ , TE 3.4 ms, FA  $30^\circ$ , 2R-R acquisition, TI 300–500 ms, and NEX2 at 24 h

following DEMRI acquisition and (3) cardiac MRI — LV volumes and function were performed on the day of DEMRI using fGRE with FOV 5 cm, slice thickness 1 mm, matrix  $256 \times 256$ , TE 5 ms, and FA  $30^\circ$ . Coronal and axial scout images were used to position a 2-dimensional imaging plane along the short axis of the LV cavity.

#### 2.4. MRI image analysis

MRI image analysis was performed as described previously [14]. Briefly, for each short-axis slice, planimetry measurements of the LV myocardium were conducted off-line by tracing the epicardial and endocardial borders at end-systole and -diastole with OsiriX software (OsiriX, open-source). The papillary muscles were considered part of the LV cavity. LV mass, LV end-diastolic volume (LVEDV), and LV end-systolic volume (LVESV) were measured to calculate the LV ejection fraction (LVEF). For infarct analysis, the MEMRI defect area and the DEMRI enhanced area were designated as scar tissue. These areas were traced in short-axis slices and integrated to determine scar volumes by MEMRI and DEMRI in matched mice hearts ( $n = 23$ ). The % MEMRI scar volume = (MEMRI defect volume/total LV mass volume)  $\times 100$  and % DEMRI scar volume = (DEMRI scar volume/total LV mass volume)  $\times 100$ . The difference between MEMRI and DEMRI defect volumes was defined as the peri-infarct volume [14].

#### 2.5. Hemodynamic monitoring

For invasive evaluation of myocardial function, the mice were investigated using an impedance-micromanometer catheter [5]. Briefly, after catheterization via the right carotid artery, a 1.4 French catheter (SPR-839, Millar Instruments, Houston, TX) was introduced into the LV and pressure–volume (PV) loops were recorded. The method was based on measuring the time-varying electrical conductance signal of two segments of blood in the left ventricle from which the total volume is calculated. Raw conductance volumes were corrected for parallel conductance by the hypertonic saline dilution method.

#### 2.6. Flow cytometry

Flow cytometry of the serum collected from the mice detected the presence of CD34<sup>+</sup> cells as described previously [14]. The serum was stained with FITC conjugated secondary antibody (1:500, Abcam, Cambridge, MA) for 30 min at room temperature. Expression of markers was determined by FACS Calibur (BD Bioscience, San Jose, CA) and FlowJo software (Tree Star, Ashland, OR) to quantify the percentage of CD34<sup>+</sup> cells. The cells were stained with mouse IgM isotype antibodies (Biolegend, San Diego, CA) to be used as the control group.

#### 2.7. Real-time PCR

Total mRNA was isolated from peri-infarct and remote areas of both the A13 ( $n = 3$ ) and NS-treated ( $n = 3$ ) myocardial tissue using RNAqueous kit (Ambion, CA). Following mRNA extraction, 1  $\mu$ g of total mRNA was reverse-transcribed into cDNA using iScript cDNA synthesis kit (Bio-Rad, CA). Real-time quantitative PCR was run on a 96 well real-time PCR thermocycler using Power SYBR Green master mix (AB), according to the manufacturer's recommendations. PCR cycle conditions were as follows: 5 min at  $95^\circ\text{C}$ , 40

cycles of 10 s at 95 °C and 1 min at 60 °C. Primer for Apelin-J receptor was synthesized by Invitrogen in forward and reverse order:

APJ receptor: ACTATGGGGCTGACAACCAG,GGCAAAGTCACCACAAAGGT. The GAPDH housekeeping gene was used as reference for the relative quantification of the gene of interest.

## 2.8. EdU labeling

To detect cell proliferation in myocardium, stem cells were labeled with 5-ethynyl-2'-deoxyuridine (EdU, Life Technologies, Grand Island, NY), a nucleoside analog of thymidine incorporated into DNA during active DNA synthesis or cell proliferation. Specifically, after the micro-osmotic pump insertion, daily intra-peritoneal injection of EdU (100µg/g body weight) to mice (n = 3 each group) was performed for 7 days to label proliferating cells. After sacrifice, formalin-fixed tissue sections were prepared for EdU-labeled cell detection using Click-iT® EdU Imaging Kit with Alexa Fluor® 488 Azide (Life Technologies, Grand Island, NY).

## 2.9. Immunohistochemistry

Paraffin sections (~4 µm thickness) of the myocardial tissue including anatomical areas were immunostained against c-kit (Cell Signaling Technology, Danvers, MA), CD-133 (Life Technologies, Grand Island, NY), Nkx2.5 (Abcam, Boston, MA), cardiac troponin I (Abcam, Boston, MA) and GATA4 (Proteintech, Chicago, IL) and examined using Leica SP2 inverted confocal microscopy system (Leica Microsystems, Wetzlar, Germany) and LSM 710 confocal microscopy system (Carl Zeiss, Oberkochen, Germany). Images were measured by Image J (provided by NIH, <http://imagej.nih.gov/ij/>). The color threshold was adjusted manually and positive signal intensity was analyzed. The number of LV cardiomyocytes and CSCs per unit volume of myocardium was determined using Velocity 3D image analysis software (PerkinElmer, Waltham, MA).

## 2.10. Histological analysis

Paraffin-embedded and sectioned (~4 µm thickness) murine hearts were prepared for histological analysis. Sections were stained with Mayer's Hematoxylin & Eosin (H&E) and Masson trichrome staining. Tissue sections were examined using an Axio Imager Z1 upright microscopy system (Carl Zeiss, Oberkochen, Germany). The area of fibrosis was measured by Image J. The ratio of the infarcted area to LV myocardial area was calculated by this method; fibrosis area/LV myocardial area × 100.

## 2.11. Cell death assay (TUNEL assay)

To detect cell death in myocardium, in situ cell death detection kit, TMR red, version 11 (Roche Applied Science, Branford, CT) has been used. All procedures have been conducted as manufacturers' instructions. Apoptotic ratio was calculated by the number of apoptotic nuclei (TUNEL positive cells)/whole number of nuclei. This signal intensity was measured by Image J and analyzed.

### 2.12. Heart weight to tibia length (HW/TL)

At the time of sacrifice, wet heart weight and left tibia length were measured to compare for any cardiac hypertrophy between the groups.

### 2.13. Statistical analysis

Data were expressed mean  $\pm$  standard error of mean. Significant differences ( $p < 0.05$ ) between two groups were tested using Mann–Whitney non-parametric test. Wilcoxon signed-rank test was used for paired samples.

## 3. Results

### 3.1. Left ventricular function and volume

At weeks 1, 2, 3, 5, and 9 post-LAD ligation (no infusion from weeks 6 to 9), LVEF was severely reduced and continued to decrease ( $23.5 \pm 1.7\%$ ,  $19.7 \pm 2.6\%$ ,  $19.1 \pm 2.3$ ,  $16.9 \pm 2.8\%$ , and  $14.1 \pm 1.8\%$ , respectively) in the saline group. However, the A13 group demonstrated sustained LVEF during the identical follow-up period, ( $21.9 \pm 3.2\%$ ,  $22.7 \pm 2.5\%$ ,  $23.2 \pm 1.2\%$ ,  $23.1 \pm 1.7\%$ , and  $23.3 \pm 2.1\%$ , respectively). The difference in the absolute LVEF value between A13 vs. saline group ( $+1.4\%$  vs.  $-9.4\%$ ,  $p = 0.03$ ) became more pronounced by week 9 (Fig. 2). However, LVEDV ( $\text{cm}^3$ ) at weeks 1, 2, 3, and 5 and at weeks 7 and 9 (extended group) in both groups did not differ while significantly decreased LVESV was seen in the A13 vs. NS groups at week 9 ( $72 \mu\text{L}$  vs.  $99 \mu\text{L}$ ,  $p < 0.05$ ).

### 3.2. Dual contrast MEMRI-DEMRI scan

MEMRI signal defect was observed consistently within the anterior, lateral, and inferoposterior regions, which corresponded to the enhanced DEMRI infarct zone (Fig. 3). Peri-infarct border zone volume was calculated by subtracting the MEMRI defect scar volume from the corresponding DEMRI (Fig. 3). The decrease in DEMRI scar volume % in the A13 vs. NS groups was significant during the 4 week duration from week 1 to week 5 ( $34.3\%$  to  $25.1\%^*$  vs.  $33.8\%$  to  $29.8\%$ ,  $*p = 0.02$ , Fig. 4A). However, MEMRI defect volume (% LV myocardium) in A13 group showed non-significant decrease when compared to saline group ( $p = 0.054$ , Fig. 4B). The resultant peri-infarct region in the A13 group showed significant decrease compared to the NS group ( $15.1\%$  to  $7.4\%^*$  vs.  $14.8\%$  to  $11.6\%$ ,  $*p = 0.02$ , Fig. 4C).

### 3.3. Pressure-volume loops

Pressure-volume (PV) loops of apelin-13 ( $n = 8$ ) and NS ( $n = 7$ ) groups were measured 5 weeks after AMI (Fig. 5). Stroke volume, LVEF, cardiac output, stroke work and  $\text{dP/dt max}$  were significantly higher in the A13 than in the NS group (Table 1). Interestingly, Tau, a standard measurement of LV relaxation function, was lower in the A13 group.

### 3.4. Flow cytometry

The serum from the A13 group showed significant mean increase in  $\text{CD34}^+$  cells compared to the NS group ( $10.1 \pm 2.3\%^*$  vs.  $0.1 \pm 0.1\%$ ,  $*p = 0.046$ , Fig. 6). This finding may indicate

A13-mediated release of the endothelial progenitor cells (EPCs) in circulation to provide sustained restoration of the peri-infarct region and LVEF.

### 3.5. Histological analysis in the A13 and NS groups after myocardial infarction

We checked for any evidence of histological difference in the A13 and NS groups at week 5 after AMI, using H&E and Masson trichrome stain (Fig. 7A–B). The histology confirmed the blue fibrotic area (Masson) in the peri-infarct region (Fig. 7B). The A13 group showed significant reduction in the fibrosis in the infarct region (A13 vs. NS,  $22.7 \pm 0.8\%$  vs.  $31.7 \pm 4.1\%$ ,  $*p = 0.002$ ).

### 3.6. Gene expression of apelin-J receptor

Comparison of the real-time PCR quantitative analysis of the remote and peri-infarct regions of the myocardial tissue in the A13 and NS groups demonstrated that the peri-infarct area in the A13 group showed significant up-regulation of the expression of apelin-J receptor (AJR) gene in comparison to the remote region of the A13 group and in comparison to both remote and peri-infarct regions of the NS group (A13 vs. NS,  $4.95 \pm 0.04^*$  vs.  $1.29 \pm 0.14$ ,  $*p = 0.049$ , Fig. 7C).

### 3.7. A13 attenuates apoptosis after AMI

The peri-infarct region of the A13 vs. NS groups was stained, employing TUNEL assay. The TUNEL positive signal (red-color) represents apoptotic cell death (Fig. 7D). The comparison of the TUNEL-stained peri-infarct tissue in the A13 vs. NS groups at week 5 demonstrated significant decrease in apoptosis ( $23.4 \pm 2.2\%$  vs.  $40.6 \pm 2.7\%$ ,  $*p = 0.021$ ).

### 3.8. Co-localization of EdU<sup>+</sup> cells with ckit, cardiac troponin I, Nkx2.5, GATA4 and CD133

EdU<sup>+</sup> cells increased significantly in the peri-infarct regions of the A13 vs. NS group as measured by Image J ( $n = 3$ ,  $21 \pm 2.4\%$  vs.  $13 \pm 2.6\%$ ,  $p = 0.006$ , Fig. 8A–D). Cardiomyocyte marker, cardiac troponin I, exhibited significant increase in the A13 vs. NS treated mice in the peri-infarct regions ( $41.5 \pm 1.9\%$  vs.  $24.3 \pm 2.5\%$ ,  $p = 0.049$ , Fig. 8A). Similarly, the cardiovascular progenitor markers, Nkx2.5 and GATA4, were significantly increased in the peri-infarct region of the A13 vs. NS group (Nkx2.5,  $60.8 \pm 8.9\%$  vs.  $29.2 \pm 3.0\%$ ,  $p = 0.049$ ; GATA4,  $48.9 \pm 3.2\%$  vs.  $20.1 \pm 4.2\%$ ,  $p = 0.049$ , Fig. 8B–C). Of the EdU<sup>+</sup> cells, 22% in the A13 group and 20% in the saline group were ckit<sup>+</sup>. Using DAPI counterstain, 87% in A13 group and 85% in saline control group showed ckit<sup>+</sup>–EdU<sup>+</sup> cells and CD133<sup>+</sup> to reflect endothelial phenotype of BMSC origin (Fig. 8E–F). This finding suggests the presence of cardiac-derived ckit<sup>+</sup> cardiac stem cells (CSC) population marked by EdU<sup>+</sup>–ckit<sup>+</sup>–cD133<sup>+</sup>, however, in a limited quantity in the heart.

### 3.9. Heart weight to tibia length (HW/TL)

Notably, there was no difference in HW/TL ratio between the 2 groups ( $0.079 \pm 0.03$  g/cm vs.  $0.080 \pm 0.02$  g/cm,  $p < 0.05$ ), suggesting no significant evidence of left ventricular hypertrophy.



## 4. Discussion

This study demonstrates for the first time that the continuous infusion of A13 following AMI preserves LV function due to salvage of the peri-infarct region. The data suggest that A13 activates both bone marrow (BM)- and cardiac-derived ckit<sup>+</sup> cardiovascular stem cells (CSC) to confer beneficial function and morphology. The cellular, molecular, and physiologic characterizations of the peri-infarct injury demonstrated modulation of APJ gene, reduction of myocardial injury, attenuation of apoptosis of the cardiomyocytes, mobilization of CD34<sup>+</sup> and BM- and cardiac-derived ckit<sup>+</sup> CSCs, and generation of favorable hemodynamic effects.

Two recent echocardiography-based studies suggest that A13 maintains cardiac function over a 2-week period [11,12]. Our current investigation provides detailed analysis of cardiac function by both cardiac MRI and invasive PV loop over an 8-week period. The data confirm the functional preservation through the 4 week treatment period and additional 4 weeks beyond the A13 treatment. This prolonged benefit addresses one of the critical issues in cardiovascular regeneration to enable a permanent and sustained functional restoration of the injured heart. Finally, the delivery timing and administration methods utilize continuous micro-osmotic infusion pump for 4 weeks to address the limited half-life of A13 [7–11].

The critical role of the peri-infarct region in the high morbidity and mortality of ischemic heart failure (HF) is well-established. Several studies have confirmed the association of the peri-infarct region with ventricular arrhythmias and remodeling, which was reduced significantly with revascularization of the injured region [17–19,20–22]. Thus, a precise characterization of cell viability and injury in this vulnerable region is imperative. Since the non-specific distribution of gadolinium in DEMRI overestimates the scar area, MEMRI is used to delineate the live cells within the scar, which was previously deemed infarcted by DEMRI [13–14,16,23–24]. The dual contrast MEMRI-DEMRI defines the peri-infarct region at the leading edge of the DEMRI scar signal where viable but injured myocardium is present. This novel technique demonstrates that A13 attenuates the volume of the peri-infarct region by salvaging the injured but viable cardiomyocytes. Combined with these novel findings, the ex vivo data confirm the production of BM- and cardiac-derived CSCs and modification of myocardial gene expression to facilitate the salvage of the peri-infarct region and preserve LVEF.

Consistent with our findings, two studies reported the effects of apelin on stem cell mobilization following AMI [11,12]. Both studies noted that the BM-derived or apelin receptor positive cells increased within the myocardium and induced angiogenesis. Our study employs dual contrast MRI to monitor the progressive viability changes in the peri-infarct myocardium. A13 significantly increased the EdU<sup>+</sup> cells by 2-fold in the peri-infarct zone in comparison to the saline control group. Of these EdU<sup>+</sup> cells, approximately, 20% were ckit<sup>+</sup> cells, suggesting cardiac stem cell phenotype. Of these proliferating cardiac stem cells, 85% were CD-133<sup>+</sup>, indicating bone marrow origin and the remaining 15% represented EdU<sup>+</sup>-ckit<sup>+</sup>-CD133<sup>+</sup>, suggesting the presence of endogenous resident CSCs. Consistent with the recent report [25], the majority of EdU<sup>+</sup> cells in both A13 and saline groups did not co-express ckit and/or CD133, suggesting that the cardiac stem cells were



present but represented a limited quantity of this privileged sub-population. These findings may be related to the role of A13 during cardiac development as a critical gradient for migration of mesodermal cells fated to contribute to the myocardial lineage and may induce the injured cardiomyocytes to re-enter the mitotic cell division cycle [26–30]. This effect is reflected in the up-regulation of the cardiovascular progenitor markers, Nkx2.5 and GATA4, and cardiomyocyte marker, cardiac troponin I in the A13 group, which may underlie the salvage of the injured cardiomyocytes [31–32]. Finally, A13 attenuates apoptosis in the peri-infarct region significantly to salvage the injured myocardium [33]. Although the restorative effects were sustained, the modest improvement in LV function suggests that the salvage capability alone may not be sufficient to impart substantial functional restoration and point to the potential adjuvant role of A13 in HF therapy.

Clinical benefit of apelin treatment in HF patients has been reported and its translational potential of apelin on pulmonary hypertension has been investigated [34–36]. Intravenous infusion (0.1 to 3 nmol/min) of A13 in healthy subjects has caused reproducible vasodilation in forearm vascular resistance [34]. Intrabrachial infusion (0.1 to 3 nmol/min) of A13 increased cardiac index and lowered mean arterial pressure and peripheral vascular resistance in patients with HF and healthy control subject [35]. Prolonged six-hour intravenous infusion of A13 (30 nmol/min) in patients with HF caused a sustained increase in cardiac index and left ventricular ejection fraction [36]. In the [clinicaltrials.gov](https://clinicaltrials.gov) database, several recent clinical studies, examining the therapeutic efficacy of apelin administration, have been identified. These studies include the following: 1) assessment of the different methods of apelin infusion (subcutaneous vs. intravenous) on cardiac output and peripheral vascular resistance in healthy volunteers, 2) evaluation of apelin infusion in patients with idiopathic pulmonary arterial hypertension, and 3) investigation of efficacy of apelin on pulmonary hypertension in patients with chronic obstructive pulmonary disease.

In conclusion, our study provides an important clinical indication for the usage of apelin as an adjuvant therapy in HF patients undergoing cell therapy. A13 preserved and sustained cardiac function after severe myocardial injury through salvage of the peri-infarct border zone by mobilizing endogenous stem cells. The pleiotropic protective effects consisted predominantly of the proliferation of native ckit<sup>+</sup>, nonckit<sup>+</sup>, and CD34<sup>+</sup> cells of both BM and cardiac origins but also included modulation of ventricular remodeling gene expression; attenuation of apoptosis; and beneficial hemodynamic effects. Further preclinical and clinical studies are warranted to determine the therapeutic potential of A13 to salvage the peri-infarct region to attenuate the pathological sequela of heart failure and promote permanent restoration of the injured myocardium.

## Acknowledgments

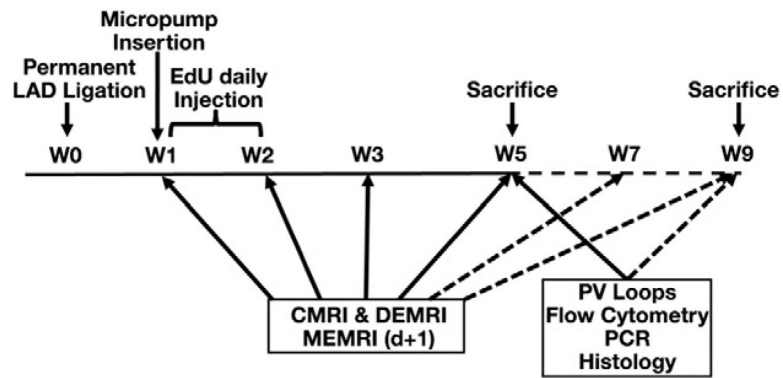
Funding sources from National Institutes of Health/National Heart, Lung, and Blood Institute: SUM1 HL113456-02 (PY), 1R01 HL097516-01 (PY), and 1K08HL097022-01 (RD) and Gachon University and Gachon University Gil Medical Center, Korea: (WJC).

## References

1. Schachinger V, Erbs S, Elsasser A, et al. Intracoronary bone marrow-derived progenitor cells in acute myocardial infarction. *N. Engl. J. Med.* 2006; 355:1210–1221. [PubMed: 16990384]

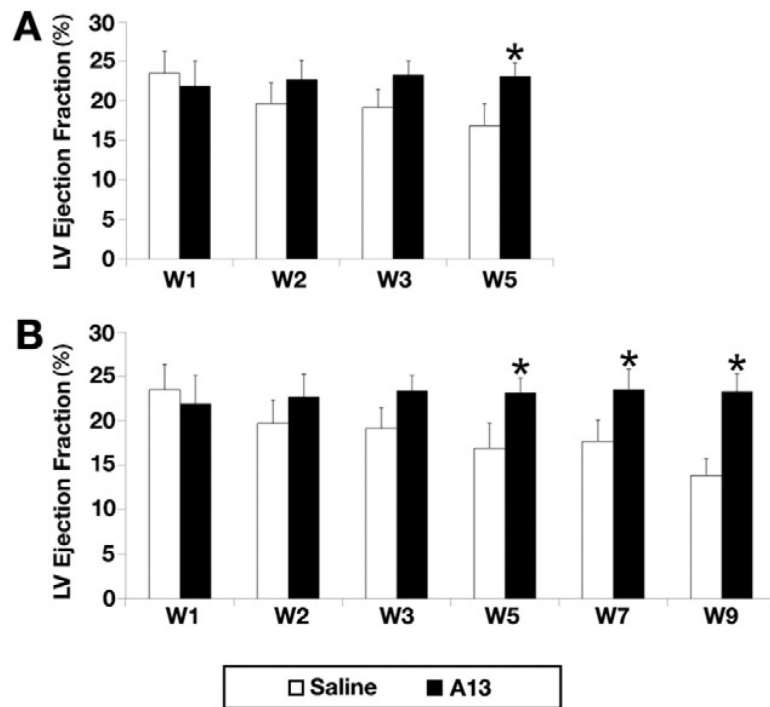
2. Makkar RR, Smith RR, Cheng K, et al. Intracoronary cardiosphere-derived cells for heart regeneration after myocardial infarction (caduceus): a prospective, randomised phase 1 trial. *Lancet*. 2012; 379:895–904. [PubMed: 22336189]
3. Bolli R, Chugh AR, D'Amario D, et al. Cardiac stem cells in patients with ischaemic cardiomyopathy (scipio): initial results of a randomised phase 1 trial. *Lancet*. 2012; 378–89:8147–8158.
4. Li TS, Cheng K, Malliaras K, et al. Direct comparison of different stem cell types and subpopulations reveals superior paracrine potency and myocardial repair efficacy with cardiosphere-derived cells. *J. Am. Coll. Cardiol*. 2012; 59:942–953. [PubMed: 22381431]
5. Beeres SL, Bengel FM, Bartunek J, et al. Role of imaging in cardiac stem cell therapy. *J. Am. Coll. Cardiol*. 2007; 49:1137–1148. [PubMed: 17367656]
6. Szokodi I. Apelin, the novel endogenous ligand of the orphan receptor apj, regulates cardiac contractility. *Circ. Res*. 2002; 91:434–440. [PubMed: 12215493]
7. Ashley EA, Powers J, Chen M, et al. The endogenous peptide apelin potently improves cardiac contractility and reduces cardiac loading in vivo. *Cardiovasc. Res*. 2005; 65:73–82. [PubMed: 15621035]
8. van Kimmenade RR, Januzzi JL Jr, Ellinor PT, et al. Utility of amino-terminal pro-brain natriuretic peptide, galectin-3, and apelin for the evaluation of patients with acute heart failure. *J. Am. Coll. Cardiol*. 2006; 48:1217–1224. [PubMed: 16979009]
9. Zeng XX, Wilm TP, Sepich DS, et al. Apelin and its receptor control heart field formation during zebrafish gastrulation. *Dev. Cell*. 2007; 12:391–402. [PubMed: 17336905]
10. Wang IN, Wang X, Ge X, et al. Apelin enhances directed cardiac differentiation of mouse and human embryonic stem cells. *PLoS One*. 2012; 7:e38328. [PubMed: 22675543]
11. Li L, Zeng H, Chen JX. Apelin-13 increases myocardial progenitor cells and improves repair of post-myocardial infarction. *Am. J. Physiol. Heart Circ. Physiol*. 2012; 303:H605–H618. [PubMed: 22752632]
12. Tempel D, de Boer M, van Deel ED, et al. Apelin enhances cardiac neovascularization after myocardial infarction by recruiting aplnr + circulating cells. *Circ. Res*. 2012; 111:585–598. [PubMed: 22753078]
13. Judd RM, Lugo-Olivieri CH, Arai M, et al. Physiological basis of myocardial contrast enhancement in fast magnetic resonance images of 2-day-old reperfused canine infarcts. *Circulation*. 1995; 92:1902–1910. [PubMed: 7671375]
14. Dash R, Chung J, Ikeno F, et al. Dual manganese-enhanced and delayed gadolinium-enhanced mri detects myocardial border zone injury in a pig ischemia-reperfusion model. *Circ. Cardiovasc. Imaging*. 2011; 4:574–582. [PubMed: 21719779]
15. Friedrich MG. Tissue characterization of acute myocardial infarction and myocarditis by cardiac magnetic resonance. *JACC Cardiovasc. Imaging*. 2008; 1:652–662. [PubMed: 19356496]
16. Amado LC, Gerber BL, Gupta SN, et al. Accurate and objective infarct sizing by contrast-enhanced magnetic resonance imaging in a canine myocardial infarction model. *J. Am. Coll. Cardiol*. 2004; 44:2383–2389. [PubMed: 15607402]
17. Tsukiji M, Nguyen P, Narayan G, et al. Peri-infarct ischemia determined by cardiovascular magnetic resonance evaluation of myocardial viability and stress perfusion predicts future cardiovascular events in patients with severe ischemic cardiomyopathy. *J. Cardiovasc. Magn. Reson*. 2006; 8:773–779. [PubMed: 17060098]
18. Yokota H, Heidary S, Katikireddy CK, et al. Quantitative characterization of myocardial infarction by cardiovascular magnetic resonance predicts future cardiovascular events in patients with ischemic cardiomyopathy. *J. Cardiovasc. Magn. Reson*. 2008; 10:17. [PubMed: 18400089]
19. Heidary S, Patel H, Chung J, et al. Quantitative tissue characterization of infarct core and border zone in patients with ischemic cardiomyopathy by magnetic resonance is associated with future cardiovascular events. *J. Am. Coll. Cardiol*. 2010; 55:2762–2768. [PubMed: 20538171]
20. St John Sutton M, Lee D, Rouleau JL, et al. Left ventricular remodeling and ventricular arrhythmias after myocardial infarction. *Circulation*. 2003; 107:2577–2582. [PubMed: 12732606]
21. Brugada J, Aguinaga L, Mont L, et al. Coronary artery revascularization in patients with sustained ventricular arrhythmias in the chronic phase of a myocardial infarction: effects on the

- electrophysiologic substrate and outcome. *J. Am. Coll. Cardiol.* 2001; 37:529–533. [PubMed: 11216974]
22. Kim RJ, Wu E, Rafael A, et al. The use of contrast-enhanced magnetic resonance imaging to identify reversible myocardial dysfunction. *N. Engl. J. Med.* 2000; 343:1445–1453. [PubMed: 11078769]
  23. Lima JA. Myocardial viability assessment by contrast-enhanced magnetic resonance imaging. *J. Am. Coll. Cardiol.* 2003; 42:902–904. [PubMed: 12957440]
  24. Delattre BM, Braunersreuther V, Hyacinthe JN, et al. Myocardial infarction quantification with manganese-enhanced mri (memri) in mice using a 3t clinical scanner. *NMR Biomed.* 2010; 23:503–513. [PubMed: 20175138]
  25. van Berlo JH, Kanisicak O, Maillet M, et al. C-kit<sup>+</sup> cells minimally contribute cardiomyocytes to the heart. *Nature.* 2014; 509(7500):337–341. [PubMed: 24805242]
  26. Scott IC, MasriB D'ALA, et al. The g protein-coupled receptor agtr1b regulates early development of myocardial progenitors. *Dev. Cell.* 2007; 12:403–413. [PubMed: 17336906]
  27. Zeng XX, WilmTP SDS, et al. Apelin and its receptor control heart field formation during zebrafish gastrulation. *Dev. Cell.* 2007; 12:391–402. [PubMed: 17336905]
  28. Ellison GM, Torella D, Dellegrottaglie S, et al. Endogenous cardiac stem cell activation by insulin-like growth factor-1/hepatocyte growth factor intracoronary injection fosters survival and regeneration of the infarcted pig heart. *J. Am. Coll. Cardiol.* 2011; 58:977–986. [PubMed: 21723061]
  29. Agbulut O, Vandervelde S, Al Attar N, et al. Comparison of human skeletal myoblasts and bone marrow-derived CD133<sup>+</sup> progenitors for the repair of infarcted myocardium. *J. Am. Coll. Cardiol.* 2004; 44:458–463. [PubMed: 15261948]
  30. Senyo SE, Steinhäuser ML, Pizzimenti CL, et al. Mammalian heart renewal by pre-existing cardiomyocytes. *Nature.* 2013; 493:433–436. [PubMed: 23222518]
  31. Kattman SJ, Huber TL, Keller GM. Multipotent flk-1<sup>+</sup> cardiovascular progenitor cells give rise to the cardiomyocyte, endothelial, and vascular smooth muscle lineages. *Dev. Cell.* 2006; 11:723–732. [PubMed: 17084363]
  32. Johkura K, Cui L, Suzuki A, et al. Survival and function of mouse embryonic stem cell-derived cardiomyocytes in ectopic transplants. *Cardiovasc. Res.* 2003; 58:435–443. [PubMed: 12757877]
  33. Cui RR, Mao DA, Yi L, et al. Apelin suppresses apoptosis of human vascular smooth muscle cells via APJ/PI3-K/Akt signaling pathways. *Amino Acids.* 2010; 39:1193–1200. [PubMed: 20495838]
  34. Japp AG, Cruden NL, Amer DA, et al. Vascular effects of apelin in vivo in man. *J. Am. Coll. Cardiol.* 2008; 52:908–913. [PubMed: 18772060]
  35. Japp AG, Cruden NL, Barnes GD, et al. Acute cardiovascular effects of apelin in humans: potential role in patients with chronic heart failure. *Circulation.* 2010; 121:1818–1827. [PubMed: 20385929]
  36. Barnes GD, Alam S, Carter G, et al. Sustained cardiovascular actions of APJ agonism during renin-angiotensin system activation and in patients with heart failure. *Circ. Heart Fail.* 2013; 6:482–491. [PubMed: 23519586]



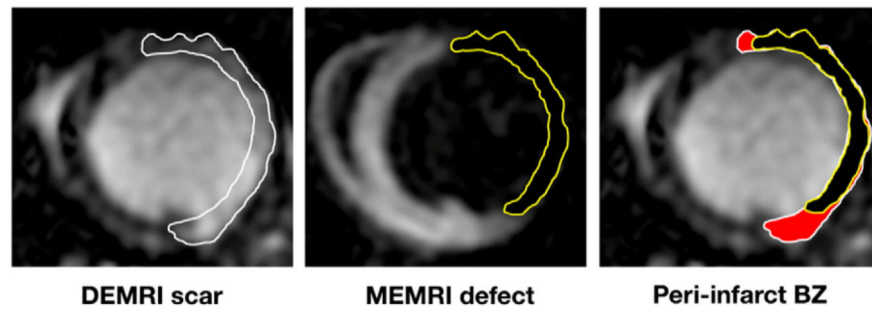
**Fig. 1.**

Study design. LAD indicates left anterior descending coronary artery; EdU, 5-ethynyl-2'-deoxyuridine; CMRI, cardiac magnetic resonance imaging; DEMRI, delayed enhanced magnetic resonance imaging; MEMRI, manganese enhanced magnetic resonance imaging; PCR, polymerase chain reaction. Broken arrow indicates the infusion-free extension period from weeks 5–9.



**Fig. 2.**

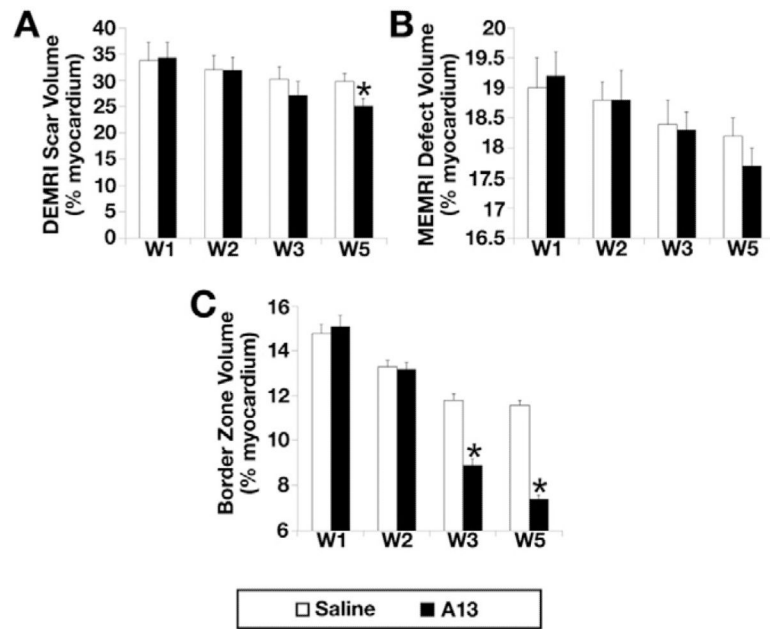
Changes in left ventricular ejection fraction (LVEF) between apelin-13 (A13) infusion (n = 16, black) and 0.9% saline infusion (n = 16, white). A. Although LVEF of 0.9% saline infusion group was significantly decreased, A13 infusion group showed preserved LVEF through 4 weeks (weeks 1–5) of infusion ( $21.9 \pm 3.2\%$  to  $23.1 \pm 1.7\%^*$  vs.  $23.5 \pm 1.7\%$  to  $16.9 \pm 2.8\%$ ,  $*p = 0.02$ ) and B. In the extended group, infusion was stopped at the end of week 5 for 4 weeks from weeks 6–9. A13 group consistently demonstrated preservation of LVEF while the saline group showed reduction of LVEF during both the 4 weeks of infusion (weeks 1–5) and the 4 weeks of extended period without infusion. LVEF change at week 9 between A13 vs. control demonstrated significant increase in A13 group ( $+1.4\%^*$  vs.  $-9.4\%$ ,  $*p = 0.03$ ).



**Fig. 3.**

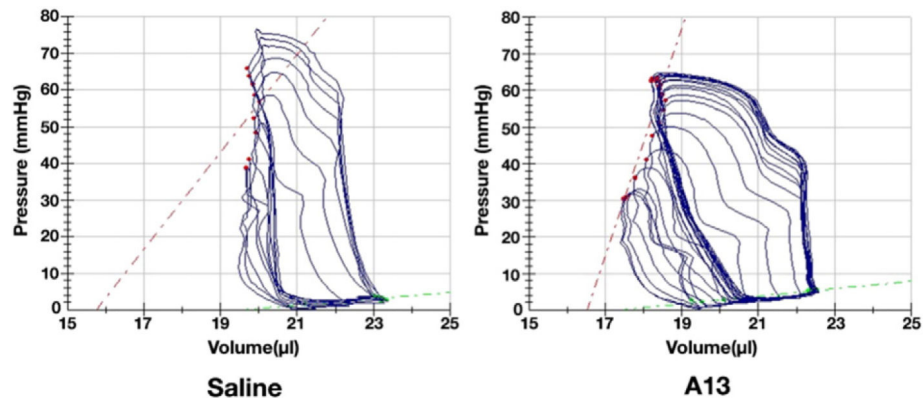
Dual contrast cardiac MR in myocardial ischemia model. A representative case of dual DEMRI-MEMRI contrast with the tracing of peri-infarct border zone area (solid red color). This area was generated by subtracting the MEMRI defect area tracing (yellow color) from the DEMRI scar area tracing (white color).



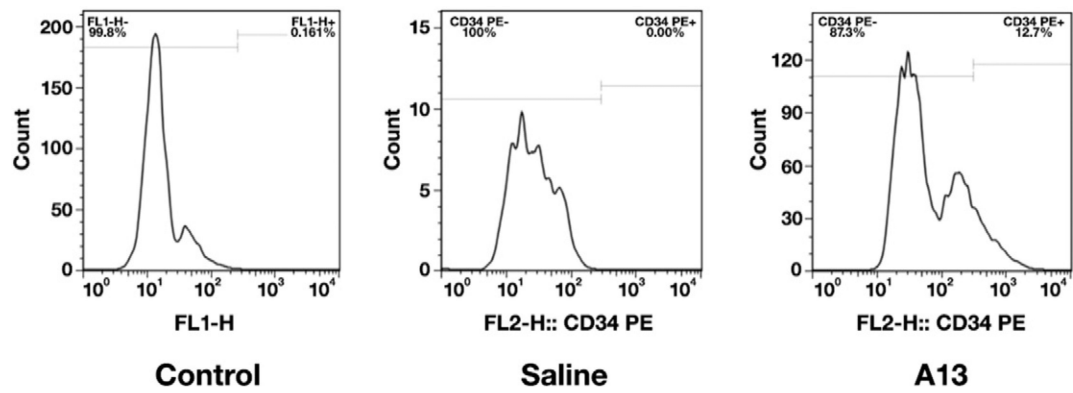


**Fig. 4.**

Changes in dual-contrast CMR parameters of A13 and NS groups during the 4-week infusion period from weeks 1 to 5. A. DEMRI scar volume (% of LV myocardium) of A13 group decreased significantly when compared to the NS group (34.3% to 25.1%\* vs. 33.8% to 29.8%,  $*p = 0.02$ ), B. MEMRI defect volume (% of LV myocardium) of A13 group showed significant decrease when compared to the NS group ( $p = 0.05$ ) and C. Peri-infarct volume (% of LV myocardium) of A13 group showed significant decrease when compared to NS group (15.1% to 7.4%\* vs. 14.8% to 11.6%,  $*p = 0.02$ ).

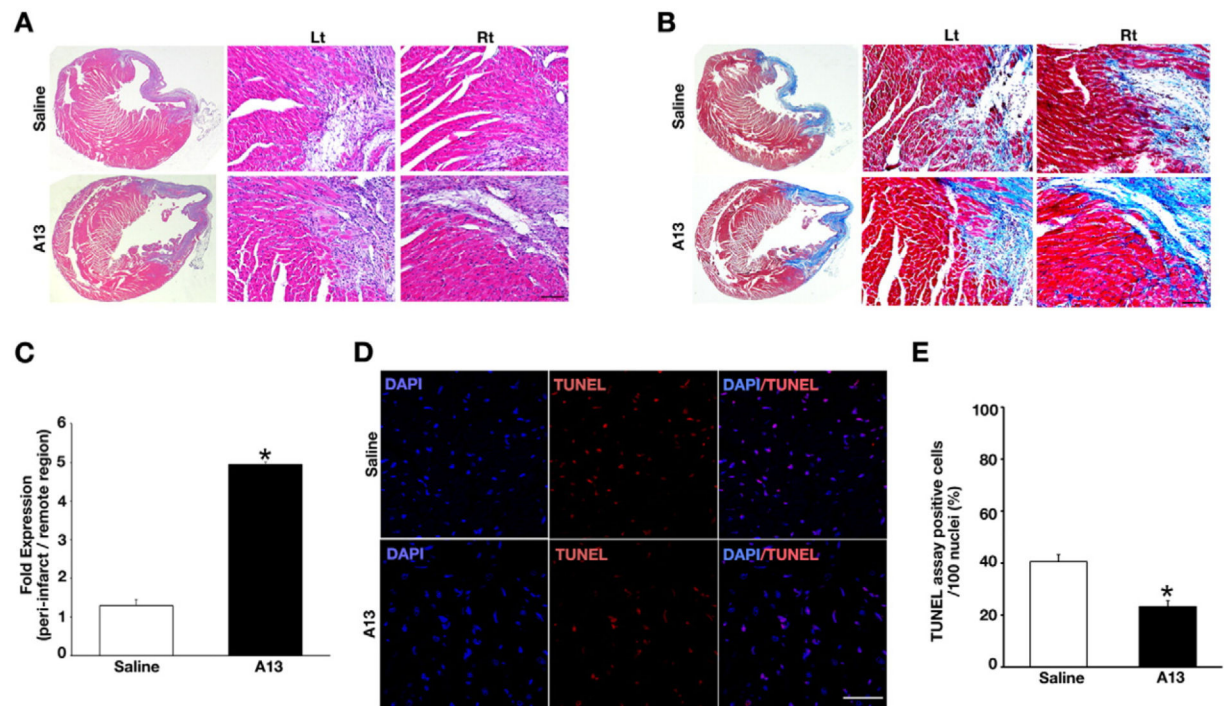


**Fig. 5.** Pressure volume loops of the saline (left) vs. apelin-13 (right) groups at week 5 after acute myocardial injury. Significantly improved end-systolic elastance (Ees) in cardiac contractility was demonstrated in the A13 vs. saline groups.

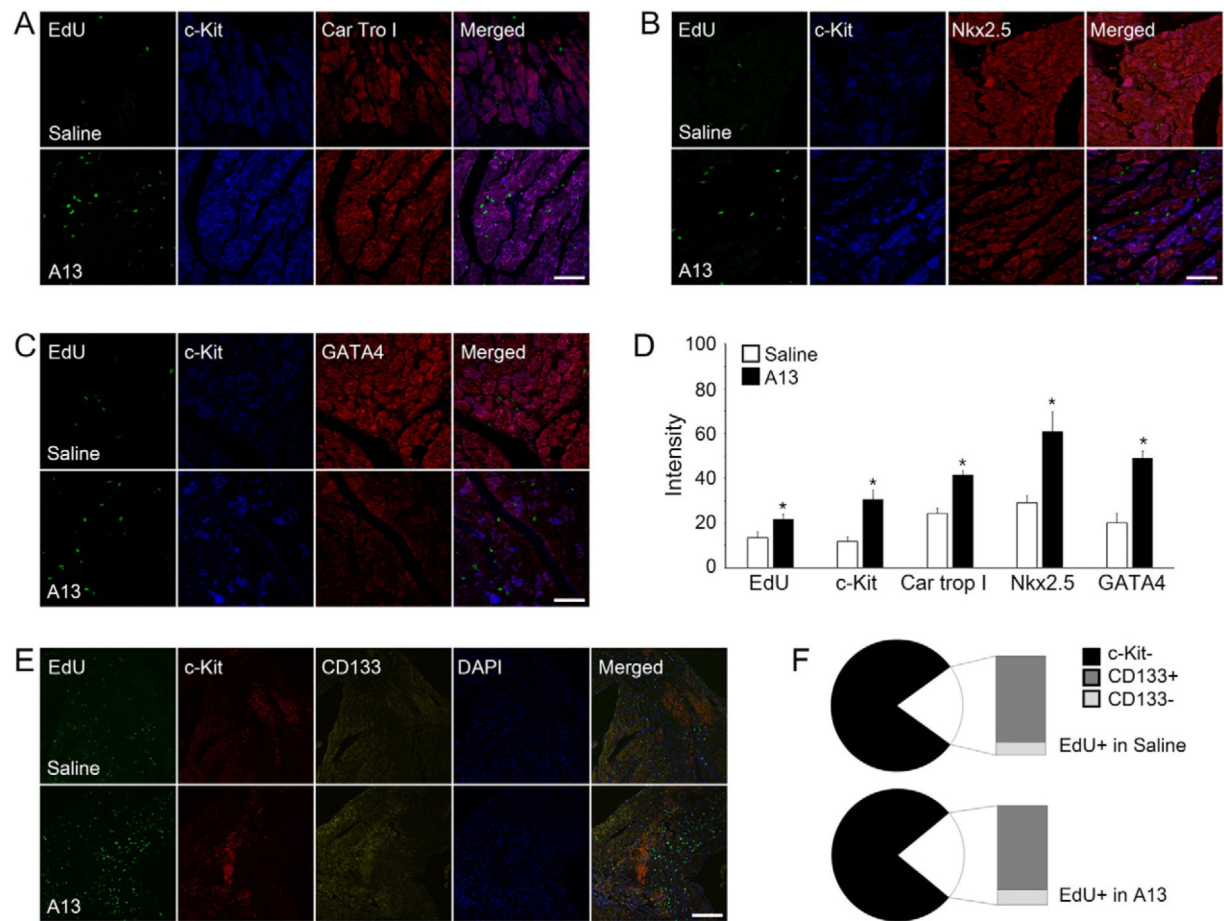


**Fig. 6.**

Flow cytometry results of CD34<sup>+</sup> cells in the peripheral blood at week 5 after acute myocardial injury. Apelin-13 group showed significantly increased CD34<sup>+</sup> cells when compared to the NS group ( $10.1 \pm 2.3\%$  vs.  $0.1 \pm 0.1\%$ ,  $p < 0.05$ ).

**Fig. 7.**

Myocardial fibrosis and apoptosis at week 5 after acute myocardial injury. A. Representative Hematoxylin and Eosin staining at week 5 after acute myocardial ischemia from A13- and NS-treated animals confirm the presence of the peri-infarct region (Lt: left peri-infarct region, Rt: right peri-infarct region). B. Tissue sections with Masson Trichrome staining at week 5 after acute myocardial injury from A13- and NS-treated animals exhibit the fibrotic blue areas in peri-infarct regions (magnification  $\times 200$  in A and B). A13 and saline group showed significant difference in the fibrosis in the infarct region (A13 vs. NS,  $22.7 \pm 0.8\%$  vs.  $31.7 \pm 4.1\%$ ,  $p = 0.002$ ). C. The real-time PCR quantitative analysis of the remote and peri-infarct regions from the A13 and NS groups demonstrates significant up-regulation in expression of APJ receptor genes in the peri-infarct regions of the A13 group, D. Representative images of TUNEL-stained heart sections of the peri-infarcted regions from saline and A13 group. Apoptotic positive cells in the peri-infarcted regions were identified by TUNEL staining (red) and whole nuclei by DAPI staining (blue, magnification  $\times 400$ ), E. Quantitative analysis of apoptotic cells in the peri-infarcted region of A13- and NS-treated groups. TUNEL positive cells are expressed as a total number per 100 nuclei in the peri-infarcted region. There was a significant decrease in apoptotic cells in the A13 vs. NS groups ( $23.4 \pm 2.2\%$  vs.  $40.6 \pm 2.7\%$ ,  $p = 0.021$ ).

**Fig. 8.**

Immunofluorescence analysis of EdU, c-kit, cardiac troponin I, Nkx2.5 and GATA4 in the peri-infarct region after saline or apelin 13 treatment. A. Triple labeled confocal microscopic image analyses were used to study the relative levels of EdU (green), c-kit (blue), and cardiac troponin I (Car Tro I, red) in the peri-infarct region after saline and apelin 13 (A13) treatment for the acute myocardial injury. B. Triple labeled confocal microscopic image analyses were used to study the relative levels of EdU (green), c-kit (blue) and Nkx2.5 (red) in the peri-infarct region. C. Triple labeled confocal microscopic image analyses were used to study the relative levels of EdU (green), c-kit (blue) and GATA4 (red) in the peri-infarct region. D. Densitometry analyses of EdU, c-kit, cardiac troponin I (Car Tro I), Nkx2.5 and GATA4 were evaluated using Image J which showed signal intensity of EdU, c-kit, Car Tro I, Nkx2.5 and GATA were significantly increased after A13 treatment vs. saline-group (EdU<sup>+</sup>,  $21 \pm 2.4\%$  vs.  $13 \pm 2.6\%$ ,  $p = 0.006$ ; c-kit<sup>+</sup>,  $30.6 \pm 4.1\%$  vs.  $11 \pm 1.9\%$ ,  $p = 0.021$ ; cardiac troponin I,  $41.5 \pm 1.9\%$  vs.  $24.3 \pm 2.5\%$ ,  $p = 0.049$ ; Nkx2.5,  $60.8 \pm 8.9\%$  vs.  $29.2 \pm 3.0\%$ ,  $p = 0.049$ ; GATA4,  $48.9 \pm 3.2\%$  vs.  $20.1 \pm 4.2\%$ ,  $p = 0.049$ ). E. Expression cellular numbers of EdU (green), c-kit (red), CD133 (orange), and DAPI (blue, nuclear marker) in the peri-infarct region were analyzed by Velocity 3D image analysis software. F. 22% (A13) and 20% (saline) of EdU<sup>+</sup> were stained with c-kit<sup>+</sup>. 87% (A13) and 85% (saline) of c-kit<sup>+</sup> cells were showed CD133<sup>+</sup>. Scale bar = 50  $\mu$ m, magnification  $\times 400$ .

**Table 1**

Pressure volume loops of saline infusion group (n = 7) and apelin-13 infusion group (n = 8) group at 5th week after acute myocardial injury.

	Saline	Apelin	<i>p</i> -Value <sup>a</sup>
HR (bpm)	356.0 ± 21.5	420.8 ± 52.1	0.39
SBP (mmHg)	75.4 ± 3.4	78.6 ± 4.2	0.39
DBP (mmHg)	54.8 ± 2.9	54.4 ± 7.3	0.83
LVESP (mmHg)	78.1 ± 6.1	84.4 ± 7.4	0.52
LVEDP (mmHg)	9.3 ± 2.7	4.7 ± 0.6	0.52
LVESV (μL)	19.4 ± 0.6	19.2 ± 0.9	0.52
LVEDV (μL)	19.9 ± 0.6	21.7 ± 0.7	0.08
SV (μL)	1.6 ± 0.1	2.9 ± 0.3	0.01 *
EF (%)	7.9 ± 0.4	13.5 ± 1.5	0.01 *
CO (μL/min)	579.1 ± 51.5	1197.4 ± 66.8	0.01 *
SW (mmHg * μL)	45.7 ± 21.4	168.3 ± 18.7	0.01 *
Ea (mmHg/μL)	50.5 ± 4.7	29.7 ± 3.9	0.06
dP/dt max (mmHg/s)	4091.7 ± 542.5	7386.0 ± 879.6	0.03 *
Tau (msec)	19.1 ± 2.9	10.9 ± 1.2	0.03 *
Ees	25.7 ± 14.4	31.9 ± 9.6	0.20
PRSW	11.7 ± 8.0	36.7 ± 6.8	0.09

Data were expressed by mean ± SEM.

<sup>a</sup>Mann-Whitney NP test.

\*  $p < 0.05$ .